

DNS of a Turbulent Lifted Ethylene/Air Jet Flame in an Autoignitive Coflow – Stabilization and Flame Structure

C. S. Yoo^{1,*}, E. S. Richardson¹, R. Sankaran², and J. H. Chen¹

*Corresponding author: csyoo@sandia.gov

¹Combustion Research Facility, Sandia National Laboratories, Livermore, CA94551-0969, USA

²National Center for Computational Sciences, Oak Ridge National Laboratories, Oak Ridge, TN 37831-6008, USA

Introduction

In many modern combustion systems such as diesel engines or direct injection stratified gasoline engines and gas turbines, fuel is injected into an environment of hot gases such that a flame may be stabilized through the recirculation of hot air and combustion products. Under such conditions, this leads to a turbulent lifted flame, and the hot environment admits the possibility of auto-ignition as a mechanism contributing to the stabilization of the flame base. In addition to auto-ignition, flame propagation and the role of large eddies have been considered as possible mechanisms for stabilization of the lifted flame base¹. In our previous 3-D direct numerical simulation (DNS) study of a turbulent lifted hydrogen/air jet flame in an autoignitive coflow, it was found that the lifted flame base forms a cycle with the passage of large-scale jet structure and the stabilization is determined by the competition between local axial velocity and auto-ignition that occurs in fuel-lean mixtures². We have recently performed 3-D DNS of a turbulent lifted ethylene/air jet flame in an autoignitive heated coflow to examine the stabilization mechanisms and flame structure of a hydrocarbon fuel jet flame.

Problem configuration

The spatially-developing turbulent lifted jet flame simulation was performed in a 3-D slot-burner configuration. Fuel issues from a central jet, which consists of 18% ethylene (C₂H₄) and 82% nitrogen by volume at an inlet temperature of $T_j = 550\text{K}$. The central jet is surrounded on either side by co-flowing heated air streams at $T_c = 1,550\text{K}$ and atmospheric pressure. The fuel jet and coflow velocities are specified as $U_j = 204\text{ m/s}$ and $U_c = 20\text{ m/s}$, and the fuel jet width, H , is 2 mm such that the jet Reynolds number, $Re_j (= HU_j/\nu)$, is approximately 10,000. The computational domain is $15H \times 20H \times 3H$ in the streamwise, x , transverse, y , and spanwise, z , directions with $2025 \times 1600 \times 400$ grid points. A uniform grid spacing of $15\mu\text{m}$ is used in the x - and z -directions, while an algebraically stretched mesh is used in the y -direction.

The compressible Navier-Stokes, species continuity, and total energy equations were solved using the Sandia DNS code, S3D, with a 4th-order Runge-Kutta method for time integration and an 8th-order central differencing scheme for spatial discretization. We adopted a reduced ethylene/air kinetic mechanism which consists of 22 species and 18 global reaction steps (T. Lu and C. K. Law, private communication, 2007). Nonreflecting inflow/outflow boundary conditions³ were used in the x - and y -directions and periodic boundary conditions were applied in the homogeneous z -direction. Based on the fuel jet velocity and the streamwise domain length, a jet time, $\tau_j = L_x/U_j$, is approximately 0.15ms. To obtain a stationary lifted flame while saving computational cost, a simulation with a grid resolution of $40\mu\text{m}$ was first performed through $10\tau_j$. The solution from that simulation was then interpolated to $15\mu\text{m}$ and used as an initial condition for the fully resolved simulation. The solution was advanced at a constant time-step of 5ns through $1.0\tau_j$. The fine-mesh simulation was performed on the Cray XT4 at Oak Ridge National Laboratories and required 2.0 million CPU-hours running for approximately 3 days on 30,000 processors.

Results and Discussion

Figure 1 shows isocontours of temperature, heat release rate, and OH mass fraction on the stoichiometric mixture fraction isosurface, $\xi_{st} = 0.2741$. Downstream of the high scalar dissipation region, temperature starts to increase at $x/H = 6$, following the increase in the heat release rate. The downstream development of the reacting planar jet flame is manifested in the profiles of the Favre mean axial velocity and the axial evolution of the jet half-width, $\delta_{1/2}$, the Favre mean temperature, and the centerline axial velocity presented in Fig. 2. Note that the axial velocity profile becomes self-similar downstream of $x/H = 7$, and $\delta_{1/2}$ increases faster than the rate at which the centerline axial velocity decreases. This is because $\delta_{1/2}$ increases as the shear layer develops right after the fuel jet nozzle, but the mean velocity does not change significantly due to thermal expansion and turbulent mixing. Global characteristics of the lifted flame represented by the Favre mean temperature and heat release rate are presented in Figure 3. Unlike the

hydrogen/air lifted jet flame¹, the mean heat release rate starts to increase in the middle of the shear layer. This is attributed not only to the large stoichiometric mixture fraction of the present flame relative to the hydrogen flame, but also to differences in the ignition characteristics of an ethylene/air mixture.

The stabilization mechanism of the present ethylene/air lifted jet flame is further investigated by tracking Lagrangian fluid particles for several flow through times. Tracer particle methods are commonly used to gain fundamental understanding of intermittent flow and flame physics⁴. The particles will provide the time history of the aero-thermo-chemical conditions that a given fluid parcel undergoes while being advected through the domain. In particular, it will provide the temporal trajectory of a given localized ignition site as it traverses oncoming turbulence intermittency, thus providing valuable lagrangian velocity-scalar statistics for models of autoignitive flows.

References

1. K. M. Lyons, *Prog. Energy Combust. Sci.* **33**, 211–231, 2007.
2. C. S. Yoo, R. Sankaran, and J. H. Chen, *J. Fluid Mech.*, submitted, 2008.
3. C. S. Yoo and H. G. Im, *Combust. Theory Modelling* **11**, 259–286, 2007.
4. P. Sripakagorn, G. Kosaly, and J. J. Riley, *Combust. Flame* **136**, 351–363, 2004.

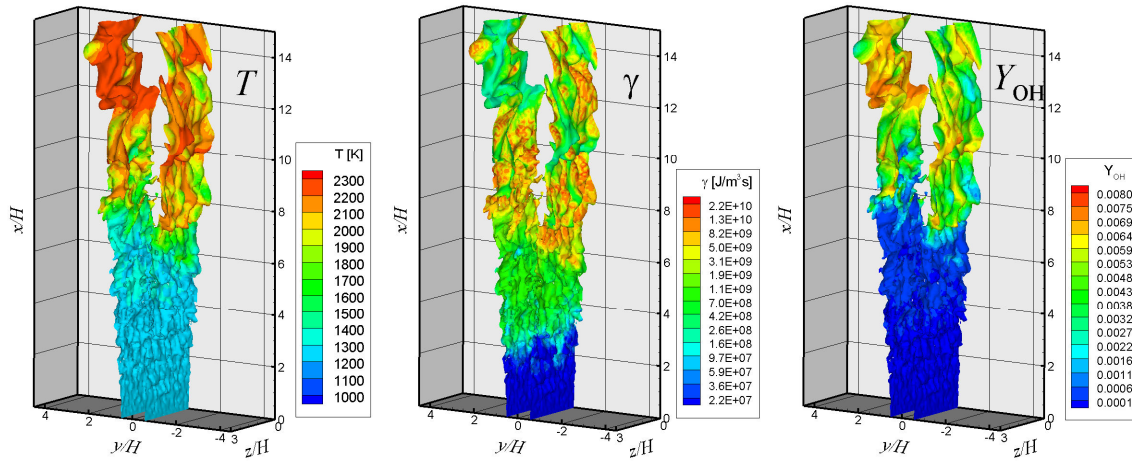


Figure 1. Instantaneous isocontours of temperature, heat release rate, and OH mass fraction on the stoichiometric mixture fraction isosurface, ξ_{st} .

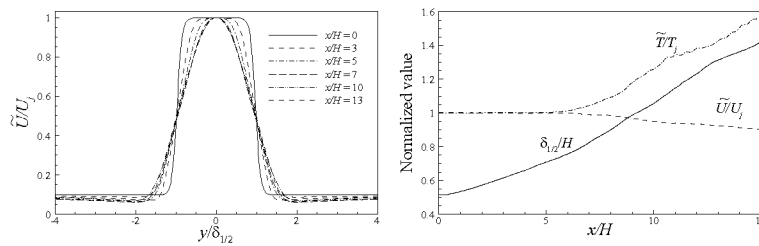


Figure 2. Profiles of the Favre mean axial velocity at different axial locations (left), and axial evolution of the jet half-width and Favre means of temperature and axial velocity at the centerline (right).

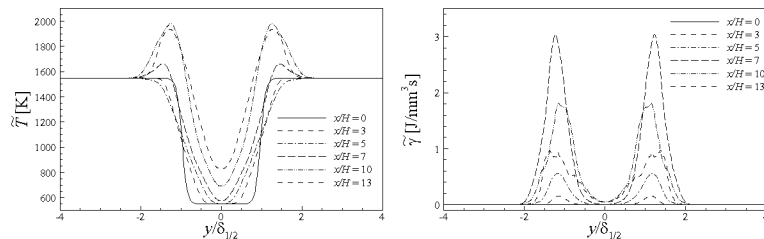


Figure 3. Profiles of the Favre means of temperature (left) and heat release rate (right) at different axial locations.